

# 1 Introduction to Carbon-Based Nanostructures

---

Carbon is a truly unique chemical element. It can form a broad variety of architectures in all dimensions, both at the macroscopic and nanoscopic scales. During the last 20+ years, brave new forms of carbon have been unveiled. The family of carbon-based materials now extends from  $C_{60}$  to carbon nanotubes, and from old diamond and graphite to graphene. The properties of the new members of this carbon family are so impressive that they may even redefine our era. This chapter provides a brief overview of these carbon structures.

## 1.1 Carbon Structures and Hybridizations

Carbon is one of the most versatile elements in the periodic table in terms of the number of compounds created from it, mainly due to the types of bonds it may form (single, double, and triple bonds) and the number of different atoms it can join in bonding. When we look at its ground state (lowest energy) electronic configuration ( $1s^2 2s^2 2p^2$ ), carbon is found to possess two core electrons ( $1s$ ) that are not available for chemical bonding and four valence electrons ( $2s$  and  $2p$ ) that can participate in bond formation (Fig. 1.1(a)). Since two unpaired  $2p$  electrons are present, carbon should normally form only two bonds in its ground state.

However, carbon should maximize the number of bonds formed because chemical bond formation will induce a decrease of system energy. Consequently, carbon will rearrange the configuration of the valence electrons. Such a rearrangement process is called *hybridization*, where only  $2s$  and  $2p$  electrons are affected. Indeed, one  $2s$  electron will be promoted into an empty  $2p$  orbital, thus forming an excited state (Fig. 1.1(b)). Carbon will thus hybridize from this excited state, being able to form at most four bonds.

One possible hybridization scheme consists in mixing the four atomic orbitals (one  $2s$  orbital + three  $2p$  orbitals), leading to the formation of four  $sp^3$  hybrid orbitals, each filled with only one electron (Fig. 1.1(c)). In order to minimize repulsion, these four hybrid orbitals optimize their position in space, leading to a tetrahedral geometry where four  $\sigma$  bonds are formed with carbon neighbors, each at an angle of  $109.5^\circ$  to each other. Methane ( $CH_4$ ) is the typical molecule that satisfies this specific bonding arrangement. Diamond is the three-dimensional carbon allotropic form where the

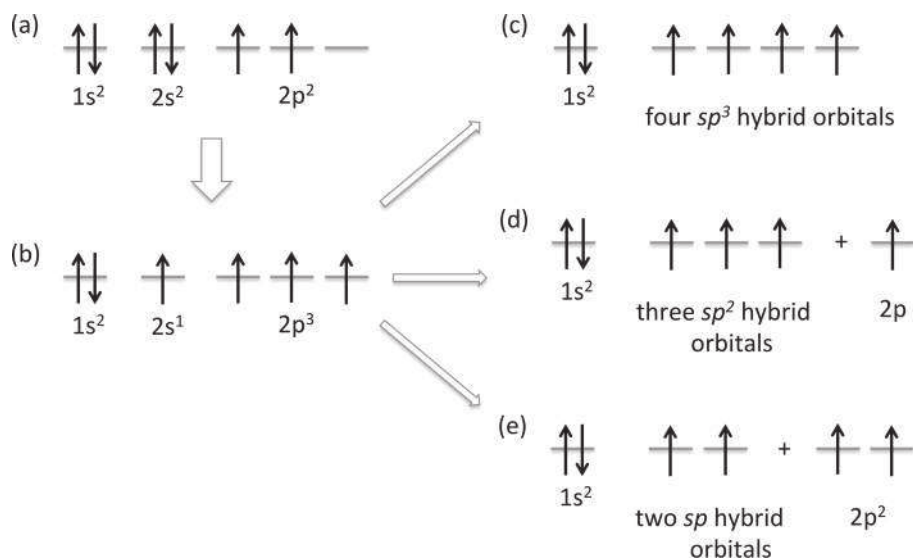


**Figure 1.1** Electronic configurations of carbon: (a) ground state; (b) excited state; (c)  $sp^3$  hybridization; (d)  $sp^2$  hybridization; and (e)  $sp$  hybridization.

atoms are arranged in a variation of the face-centered cubic crystal structure called a diamond lattice (Fig. 1.2(a)). In diamond, all carbon atoms are in the  $sp^3$  hybridization and are connected by  $\sigma$  bonds (due to the overlapping between two hybrid orbitals, each containing one electron) to four nearest neighbors with a bond length of 1.56 Å. Diamond (from the ancient Greek  $\alpha\delta\alpha\mu\alpha\sigma$  – *adamas* “unbreakable”) is renowned as a material with extreme mechanical properties originating from the strong  $sp^3$  covalent bonding between its atoms. In particular, diamond exhibits one of the highest hardness values, has an extremely high thermal conductivity, is an electrical insulator with a bandgap of  $\sim 5.5$  eV, and is transparent to visible light (Hemstreet et al. 1970).

Another possible hybridization scheme consists in mixing three atomic orbitals among the four (one  $2s$  orbital + two  $2p$  orbitals), leading to the formation of three  $sp^2$  hybrid orbitals, each filled with only one electron (Fig. 1.1(d)). Again, the three  $sp^2$  hybrid orbitals will arrange themselves in order to be as far apart as possible, leading to a trigonal planar geometry where the angle between each orbital is  $120^\circ$ . The remaining  $p$ -type orbital will not mix and will be perpendicular to this plane. In such a configuration, the three  $sp^2$  hybrid orbitals will form  $\sigma$  bonds with the three nearest neighbors and the side-by-side overlap of the unmixed pure  $p$  orbitals will form  $\pi$  bonds between the carbon atoms, accounting for the carbon–carbon double bond. Ethylene ( $C_2H_4$ ) and aromatic molecules like benzene ( $C_6H_6$ ) are typical examples of  $sp^2$  hybridization.

Graphite is a three-dimensional crystal made of stacked layers consisting of  $sp^2$  hybridized carbon atoms (Fig. 1.2(b)); each carbon atom is connected to another three making an angle of  $120^\circ$  with a bond length of 1.42 Å. This anisotropic structure

## 1.1 Carbon Structures and Hybridizations

3

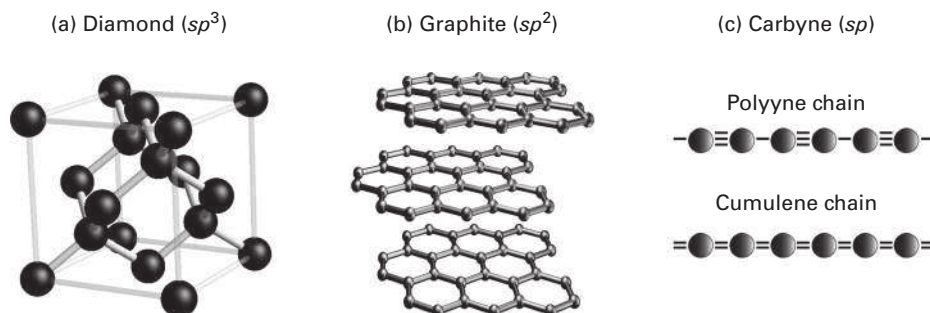


**Figure 1.2** Carbon structures exhibiting different hybridizations: (a) diamond ( $sp^3$ ); (b) graphite ( $sp^2$ ); and (c) carbyne ( $sp$ ).

clearly illustrates the presence of strong  $\sigma$  covalent bonds between carbon atoms in the plane, while the  $\pi$  bonds provide the weak interaction between adjacent layers in the graphitic structure. Graphite (from the ancient Greek  $\gamma\rho\alpha\phi\omega$  – *graphó* “to write”) is well known for its use in pencils because of its ability to mark surfaces as a writing material, due to nearly perfect cleavage between basal planes related to the anisotropy of bonding. Under standard conditions (ordinary temperatures and pressures), the stable form of carbon is *graphite*. Unlike diamond, graphite is a popular lubricant, an electrical (semi-metal) and thermal conductor, and reflects visible light. *Natural* graphite occurs in two crystal structures: Bernal (hexagonal) (Bernal 1924) and rhombohedral (Lipson & Stokes 1942) structures that are characterized by different stackings of the basal planes, ...*ABABAB*... and ...*ABCABC*..., respectively. The hexagonal and rhombohedral structures belong to the  $P6_3/mmc$  ( $D_{6h}^4$ ) and  $R\bar{3}m$  ( $D_{3d}^5$ ) space groups, respectively. Samples usually contain no more than 5–15% rhombohedral structure intermixed with Bernal form, and sometimes, disordered graphite (Lipson & Stokes 1942). These disordered graphitic forms, such as pregraphitic carbon or turbostratic graphite, are mainly composed of randomly oriented basal carbon sheets. However, pure graphite crystals can be found naturally and can also be artificially synthesized by thermolytic processes, such as the production of highly oriented pyrolytic graphite (HOPG) (Moore 1974).

The last possible hybridization consists in mixing two atomic orbitals (one  $2s$  orbital + one  $2p$  orbital) of the four, leading to the formation of two  $sp$  hybrid orbitals, each filled with only one electron (Fig. 1.1(e)). The geometry that results is linear with an angle between the  $sp$  orbitals of  $180^\circ$ . The two remaining  $p$ -type orbitals, which are not mixed, are perpendicular to each other. In such a configuration, the two  $sp$  hybrid orbitals will form  $\sigma$  bonds with the two nearest neighbors and the side-by-side overlap of the two unmixed pure  $p$  orbitals will form  $\pi$  bonds between the carbon atoms, accounting for the carbon–carbon triple bond (which is thus composed of one  $\sigma$  bond and two  $\pi$  bonds). Acetylene ( $H-C\equiv C-H$ ) is the typical linear molecule that satisfies this specific bonding arrangement. Carbon also has the ability to form one-dimensional chains, called carbynes (Fig. 1.2(c)), that are traditionally classified as *cumulene* (monoatomic chains

with double bonds,  $\cdots = \text{C} = \text{C} = \cdots$ ) or *polyynes* (dimerized chains with alternating single and triple bonds,  $\cdots - \text{C} \equiv \text{C} - \cdots$ ). While  $sp^2$  and  $sp^3$  carbon-based structures have been widely characterized, the synthesis of carbynes has been a challenge for decades due to the high reactivity of chain ends and a strong tendency to interchain crosslinking (Heimann et al. 1999). Linear carbon chains consisting of a few tens of atoms were first synthesized via chemical methods (Cataldo 2005) by stabilizing the chain ends with nonreactive terminal groups (Kavan & Kastner 1994; Lagow et al. 1995). However, these systems consist of a mixture of carbon and other chemical elements, and the synthesis of carbynes in a pure carbon environment has only recently been achieved via supersonic cluster beam deposition (Ravagnan et al. 2002, 2007) and via electronic irradiation of a single graphite basal plane (graphene) inside a transmission electron microscope (Jin et al. 2009; Meyer et al. 2008).

## 1.2 Carbon Nanostructures

Carbon nanomaterials also reveal a rich polymorphism of various allotropes exhibiting each possible dimensionality: fullerene molecule (0D), nanotubes (1D), graphite platelets and graphene ribbons (2D), and nano-diamond (3D) are selected examples (Terrones et al. 2010). Because of this extraordinary versatility of nanomaterials exhibiting different physical and chemical properties, carbon nanostructures are playing an important role in nanoscience and nanotechnology.

Carbon nanoscience started with the discovery of  $\text{C}_{60}$  Buckminsterfullerene (Kroto et al. 1985). This cage-like molecule of 7 Å diameter contains 60 carbon atoms laid out on a sphere (Fig. 1.3(a)). The structure of the  $\text{C}_{60}$  Buckminsterfullerene consists of a truncated icosahedron with 60 vertices and 32 faces (20 hexagons and 12 pentagons where no pentagons share a vertex) with a carbon atom at the vertex of each polygon and a bond along each polygon edge (Fig. 1.3(a)). Each carbon atom in the structure is bonded covalently with three others ( $sp^{2+\delta}$  hybridization;  $\delta$  is due to the curvature) with an average bond length of 1.46 Å within the five-member rings (single bond) and 1.4 Å for the bond connecting five-member rings (the bond fusing six-member rings). The number of carbon atoms in each fullerene cage can vary. Indeed, fullerene molecules are generally represented by the formula  $\text{C}_n$ , where  $n$  denotes the number of carbon atoms present in the cage. Anyway, the  $\text{C}_{60}$  nano-soccer ball (or *buckyball*) is the most stable and well-characterized member of the fullerene family. The name of these  $\text{C}_n$  molecules was derived from the name of the noted inventor and architect Buckminster Fuller since  $\text{C}_n$  resembles his trademark geodesic domes. The  $\text{C}_{60}$  molecule is still dominating fullerene research and stimulating the creativity and imagination of scientists, and has paved the way for a whole new chemistry and physics of nanocarbons (Dresselhaus et al. 1996).

Soon after, in 1988, graphitic onions – of which the first electron microscope images were reported by Sumio Iijima in 1980 (Harris 1999) – were suggested to

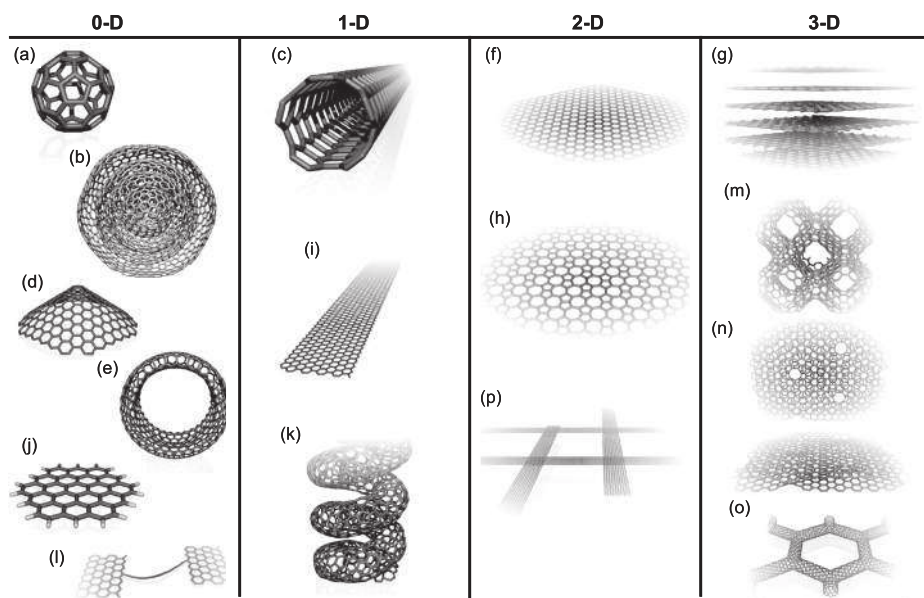


**Figure 1.3** Atomistic models of various  $sp^2$ -like hybridized carbon nanostructures exhibiting different dimensionalities, 0D, 1D, 2D, and 3D: (a)  $C_{60}$ : Buckminsterfullerene; (b) nested giant fullerenes or graphitic onions; (c) carbon nanotube; (d) nanocones or nanohorns; (e) nanotoroids; (f) graphene surface; (g) 3D graphite crystal; (h) Haeckelite surface; (i) graphene nanoribbons; (j) graphene clusters; (k) helicoidal carbon nanotube; (l) short carbon chains; (m) 3D Schwarzschild crystals; (n) carbon nanofoams (interconnected graphene surfaces with channels); (o) 3D nanotube networks, and (p) nanoribbon 2D networks. Reproduced from Terrones et al. (2010)

be nested icosahedral fullerenes ( $C_{60}@C_{240}@C_{540}@C_{960}...$ ) (Kroto & McKay 1988) containing only pentagonal and hexagonal carbon rings (Fig. 1.3(b)). In 1992, the reconstruction of polyhedral graphitic particles into almost spherical carbon onions (nested giant fullerenes) was demonstrated by Daniel Ugarte (1992) using high-energy electron irradiation inside a high-resolution transmission electron microscope (HRTEM). By analogy, the formation of  $C_{60}$  has also been very recently observed *in situ* by creating local defects in graphene upon electron irradiation in a HRTEM (Chuvilin et al. 2010). These carbon onions are quasi-spherical nanoparticles consisting of fullerene-like carbon layers enclosed by concentric graphitic shells, thus exhibiting electronic and mechanical properties different from any other carbon nanostructures due to their highly symmetric structure.

In 1976, the “ultimate” carbon fibers (later known as a multiwall carbon nanotubes), produced by a modified chemical vapor deposition (CVD) method usually used to produce conventional carbon fibers, were observed using TEM (Oberlin et al. 1976). However, the emergence of carbon nanotubes (CNTs) really came in 1991 after the  $C_{60}$  discovery. Indeed, “graphite microtubules,” multiwall nanotubes (MWNTs) produced via an arc discharge between two graphite electrodes in an inert atmosphere

(same method for producing fullerenes), were first characterized using HRTEM (Iijima 1991), thus confirming that their atomic structures consisted of nested graphene nanotubes terminated by fullerene-like caps. A couple of years later, in 1993, single-wall carbon nanotubes – SWNTs, Fig. 1.3(c) – were synthesized using the same carbon arc technique in conjunction with metal catalysts (Bethune et al. 1993; Iijima & Ichihashi 1993). CNTs are allotropic forms of carbon characterized by a long and hollow cylindrical-shaped nanostructure with a length-to-diameter ratio that may reach  $10^8$  (Zheng et al. 2004), which is significantly larger than for any other one-dimensional material. Carbon nanotubes are frequently considered as members of the fullerene family, since their ends may be capped with a buckyball hemisphere. The cylinder walls are formed by one-atom-thick sheets of carbon rolled up at specific and discrete *chiral* angles. Both the nanotube diameter and this rolling angle lead to specific properties; for example, a SWNT may behave as a metal or a semiconductor depending on its geometry (Saito et al. 1998), as described in detail in Chapter 2. Due to long-range weak interactions (van der Waals and  $\pi$ -stacking), individual nanotubes naturally align into *ropes* or *bundles* (Thess et al. 1996). These carbon nanotubes exhibit unusual properties which are extremely valuable for nanotechnology, electronics, mechanics, optics, and other fields of materials science. In particular, owing to their extraordinary mechanical properties, electrical and thermal conductivity, carbon nanotubes find applications as additives (primarily carbon fiber) in composite materials, as for instance, in baseball bats, golf clubs, or car parts (Dresselhaus et al. 2001).

After these consecutive discoveries of the fullerenes and carbon nanotubes, other graphitic-like nanostructures were successfully produced, observed, and accurately characterized using various experimental techniques. The topologies associated with these new carbon nanostructures include nanocones (Fig. 1.3(d)) (Krishnan et al. 1997), nanopeapods (Smith et al. 1998), nanohorns (Fig. 1.3(d)) (Iijima et al. 1999), and carbon rings or toroids (Fig. 1.3(e)) (Liu et al. 1997).

The fundamental building block in all these carbon nanostructures (except for  $sp^3$  nanodiamond) relies on the theoretical concept of the two-dimensional crystalline allotrope of carbon called *graphene* (Fig. 1.3(f)). Indeed, graphene is the name given to the ideally perfect infinite one-atom-thick planar sheet of  $sp^2$ -bonded carbon atoms, densely packed in a honeycomb crystal lattice (Boehm et al. 1962). This ideal two-dimensional solid has thus been widely employed as a useful theoretical concept to describe the properties of many carbon-based materials, including graphite (where a large number of graphene sheets are stacked; see Fig. 1.3(g)) (Wallace 1947), nanotubes (where graphene sheets are rolled up into nanometer-sized cylinders; see Fig. 1.3(c)), large fullerenes (where graphene sheets, according to Euler's theorem, contain at least 12 pentagons displaying a spherical shape; see Fig. 1.3(a–b)), and ribbons (where graphene is cut into strips; see Fig. 1.3(i)) (Li et al. 2008). Actually, planar graphene itself was presumed not to exist in the free state, being unstable with respect to the formation of curved structures such as soot, fullerenes, and nanotubes. However, in 2004, graphene samples were synthesized either by mechanical exfoliation (repeated peeling or micromechanical cleavage, known as the “scotch tape method”) of bulk



graphite (highly oriented pyrolytic graphite) (Novoselov et al. 2004, 2005) or by epitaxial growth through thermal decomposition of SiC (Berger et al. 2006). The relatively easy production of graphene using the scotch tape method and the transfer facility of a single atomic layer of carbon from the *c*-face of graphite to a substrate suitable for the measurement of its electrical properties have led to a renewed interest in what was considered to be a prototypical, yet theoretical, two-dimensional system. Graphene displays unusual electronic properties arising from confinement of electrons in two dimensions and peculiar geometrical symmetries. Indeed, old theoretical studies of graphene (Wallace 1947) reveal that the specific linear electronic band dispersion near the Brillouin zone corners (Dirac point) gives rise to electrons and holes that propagate as if they were massless Dirac fermions, with a velocity of the order of a few hundredths of the velocity of light. Charge excitations close to the Fermi level can thus be formally described as massless relativistic particles obeying a Dirac equation, whereas a new degree of freedom reflecting inherent symmetries (sublattice degeneracy) appears in the electronic states: the *pseudospin*. Because of the resulting pseudospin symmetry, electronic states turn out to be particularly insensitive to external sources of elastic disorder (topological and electrostatic defects) and, as a result, charge mobilities in graphene layers as large as  $10^5 \text{ cm}^2 \text{ V}^{-1} \text{ s}^{-1}$  have been reported close to the Dirac point (Novoselov et al. 2004). In addition, in suspended graphene, the minimum conductivity at the Dirac point approaches a universal (geometry independent) value of  $4e^2/h$  at low temperature (Du et al. 2008). Low-temperature electron mobility approaching  $2 \times 10^5 \text{ cm}^2 \text{ V}^{-1} \text{ s}^{-1}$  has been measured for carrier density below  $5 \times 10^9 \text{ cm}^{-2}$ . Such values cannot be attained in conventional semiconductors such as silicon or germanium. In addition, graphene has been demonstrated to exhibit anomalous quantum transport properties such as an integer quantum Hall effect (Novoselov et al. 2005; Zhang et al. 2005), and also one of the most exotic and counterintuitive consequences of quantum electrodynamics: the unimpeded penetration of relativistic particles through high and wide potential barriers, known as the Klein paradox (Katsnelson et al. 2006). These discoveries have stirred a lot of interest in the scientific community as well as in the international media. The excitement behind this discovery has two main driving forces: basic science and technological implications (Geim & Novoselov 2007). Because of its high electronic mobility, structural flexibility, and capability of being tuned from *p*-type to *n*-type doping by the application of a gate voltage, graphene is considered a potential breakthrough in terms of carbon-based nanoelectronics.

All these outstanding properties of the graphene sheet have heavily stimulated the discovery of new, closely-related planar carbon-based nanostructures with  $sp^2$  hybridization, such as bilayer graphene, trilayer graphene, few-layer graphene, and graphene nanoribbons; these nanostructures that have subsequently emerged, each having novel and unusual properties that are different from those of both graphene and graphite. Whenever these structures exhibit ...*ABABAB*... or ...*ABCABC*... stackings, they are considered as graphitic stacks. In fact, this distinction is made because it has been demonstrated that the properties of graphene can be recovered in systems with several  $sp^2$ -hybridized carbon layers when stacking disorder is introduced.

Theoretical works have also suggested the possibility of stable, flat  $sp^2$ -hybridized carbon sheets containing pentagons, heptagons, and hexagons, termed pentaheptites (2D sheets containing heptagons and pentagons only) (Crespi et al. 1996) or Haeckelites (2D crystals containing pentagons, heptagons and/or hexagons, see Fig. 1.3(h)) (Terrones et al. 2000). These planar structures are intrinsically metallic and could exist in damaged or irradiated graphene. However, further experiments are needed in order to both produce and identify them successfully.

When infinite perfect graphene crystals become finite, borders and boundaries appear, implying the presence of carbon atoms that exhibit a coordination below three at the edges. Among these graphene-based nanostructures are nanoribbons (Fig. 1.3(i)) and nanoclusters (Fig. 1.3(j)). In general, a graphene nanoribbon (GNR) is defined as a 1D  $sp^2$ -hybridized carbon crystal with boundaries, which possesses a large aspect ratio (Fig. 1.3(i)). Edge terminations could be armchair, or zigzag, or even a combination of both. The graphene cluster concept arises when the dimensionality is lost and no periodicity is present (Fig. 1.3(j)). Finally, long carbon chains either with alternating single–triple or with double bonds (Fig. 1.2(c)) are also considered as a 1D nanosystem as already briefly described in the previous section.

Finally, Schwarzites are hypothetical graphitic ( $sp^2$  hybridization) three-dimensional crystals obtained by embedding non-hexagonal carbon rings (Fig. 1.3(m)), thus spanning two different space groups in which the most symmetrical cases belong to cubic Bravais lattices (Terrones & Terrones 2003). These 3D carbon-based nanostructures can be visualized as nanoporous carbon (Fig. 1.3(n)), exhibiting nanochannels. From a theoretical point of view, these nanoporous carbon materials have been suggested to have outstanding performance in the storage of hydrogen due to their large surface area (Kowalczyk et al. 2007). Another type of 3D array of nanocarbons consists of nanotube networks (Fig. 1.3(o)), which have been predicted to exhibit outstanding mechanical and electronic properties, besides having a large surface area (e.g., 3600 m<sup>2</sup>/g) (Romo-Herrera et al. 2006). Interestingly, these types of random 3D nanotube networks have been produced using CVD approaches (Lepro et al. 2007) and further theoretical and experimental studies are still required in order to achieve crystalline 3D networks.

The series of events described above and dedicated to the most important discoveries in carbon nanoscience clearly demonstrate that carbon is a fascinating element and is able to form various morphologies at the nanoscale, possessing different physicochemical properties, some of them yet unknown. In the following sections, we will concentrate on novel one- and two-dimensional  $sp^2$ -like carbon nanostructures. But before starting your trip, we recommend that you read *Guide to the Book* below.

## 1.3 Guide to the Book

This book deals with the electronic and transport properties of some of the most promising new forms of carbon ever introduced before. Chapter 2 starts by introducing the electronic properties of both pristine and defected carbon nanostructures, and



also overviews the salient electronic features under magnetic fields (Aharonov–Bohm phenomenon and Landau levels). The emphasis is on tight-binding models, though widely used effective low-energy models are also introduced. When possible, the results are commented on in the light of *ab initio* simulations. Chapter 3 overviews the electronic properties of the most important representatives of the 2D materials family other than graphene (*h*-BN, TMDs, Phosphorene, Borophene, Silicene, Germanene, Stanene, MXenes, ...), including also some review related to novel electronic and optoelectronic properties in van der Waals heterostructures.

The rest of the book is mostly dedicated to the electronic transport properties of graphene-related materials. Chapter 4 offers a general overview of the tools used later on, namely, Landauer–Büttiker and Kubo–Greenwood formalisms, together with the commonly used semiclassical Boltzmann transport equation, which presents severe limitations for the exploration of the quantum transport at the Dirac point. Most of the technical details (or tricks!) concerning the numerical implementations of such transport methods are given in dedicated appendices. The first illustrations of transport properties in disordered graphene materials are given in Chapter 5, with a starting discussion concerning the limits of ballistic transport and the peculiar Klein tunneling mechanism. The role of disorder is further discussed broadly in Chapter 6 through the use of the legendary Anderson disorder model, which is the first approach for studying the main transport length scales and conduction regimes. Weak and strong localization phenomena (including weak antilocalization) are presented and related to the nature of disorder (short- versus long-range potential). Various forms of structural disorders are then studied including monovacancies, and polycrystalline and amorphous graphene, showing how irregularities affect mean free paths and localization lengths, eventually turning the materials to a strong Anderson insulator.

Chapter 7 covers different aspects of Berry phases, magnetic field effects, and the quantum Hall regime. The chapter ends with a presentation of Haldane’s model for a quantum Hall effect without Landau levels. Chapter 8 gives an overview of spintronics in two-dimensional materials. This chapter presents some debate and open issues, as perceived by the authors, and these issues should generate a great amount of research in the next decade. In particular, graphene spintronics offers fascinating possibilities of revolutionary information processing using the spin degree of freedom. Progress toward spin gating and spin manipulation, however, demands attention and effort in revisiting the way spin diffusion and spin relaxation mechanisms are described in graphene, as these are likely to genuinely differ from conventional relaxation effects described in metals and small-gap semiconductors.

Chapter 9 gives a brief overview of quantum transport beyond DC conditions, Floquet theory for time-periodic Hamiltonians, and a succinct review of the literature on AC transport in carbon-based nanostructures. This is currently a very active field, which connects to graphene photonics and plasmonics. Many developments are expected within the next few years, and theoretical study certainly needs to be further extended. The material provided here will be very useful for those researchers interested in the field.

*Ab initio* and multiscale transport methodologies are discussed in Chapter 10. To achieve accurate transport calculations on very-large-size disordered systems, a combination of *ab initio* approach and order- $N$  transport algorithms is crucial. The presentation will provide a simple description of various possible hybrid methodologies for investigating the complex transport fingerprints of chemically or structurally disordered carbon nanotubes of graphene-based materials. Some targeted functionalities such as chemical sensing will then be discussed in detail for chemically functionalized nanotubes. Sensing is often viewed as a major application for such low-dimensional carbon-based materials. The possibilities but also limitations of these numerical approaches are illustrated in this chapter.

Some of these chapters are essentially tutorials (Chapters 1–5, 7, and 9 and Appendices A–D), offering enough material for introductory lectures at the master degree level. Others are intended to give an overview of most foundational literature in the respective fields or to shine some light on leading-edge research (Chapters 6, 8, and 10). The choice of topics, presentation, and illustrations is unavoidably biased toward the authors' own experiences, and despite the attempts to properly acknowledge the foundational papers, many citations are certainly missing. We will try to amend this in later editions.

All chapters contain a very short list of suggested material for further reading. The core tutorial chapters of this book contain lists of problems with varying levels of difficulty. Many of them are computational exercises where a *learning by doing* spirit is encouraged. Along this line, many solutions, additional exercises, and miscellaneous material, as well as computational codes, are made available online at the website:

[www.introductiontographene.org](http://www.introductiontographene.org)  
[www.cambridge.org/foatorres](http://www.cambridge.org/foatorres)



The symbol on the right will indicate that additional material is available online. The authors intend that an updated list of typos and errors will also be available there. This will be the authors' contact point with their ultimate inspiration for this enterprise: you and your fellow readers.

Finally, the interdisciplinarity of the potential readers of this book makes it impossible (and probably pointless) to develop a book that all readers can read linearly from beginning to end. This is why the authors suggest tailoring it to your own experience and objectives. Before starting, it is recommended that you get your own *Table of Instructions* from the authors' website.

## 1.4 Further Reading

- Readers may enjoy the personal accounts given in Dresselhaus (2011) and Geim (2011), where the flavor of the story behind the development of these materials is given.